

Magnetic field dependence of the threshold electric field in unconventional charge density waves

Balázs Dóra

Department of Physics, Technical University of Budapest, H-1521 Budapest, Hungary

Attila Virosztek

*Department of Physics, Technical University of Budapest, H-1521 Budapest, Hungary
and Research Institute for Solid State Physics and Optics, P.O. Box 49, H-1525 Budapest, Hungary*

Kazumi Maki

Department of Physics and Astronomy, University of Southern California, Los Angeles, California 90089-0484

(Received 10 May 2001; revised manuscript received 15 October 2001; published 11 April 2002)

Many experiments suggest that the unidentified low-temperature phase of α -(BEDT-TTF)₂KHg(SCN)₄ is most likely unconventional charge density wave (UCDW). To further extend this identification we present our theoretical study of the threshold electric field of UCDW in a magnetic field. The magnetic field-temperature phase diagram is very similar to those in a d -wave superconductor. The optical conductivity shows clear features characteristic to both UDW and magnetic field. We find a rather strong field dependence of the threshold electric field, which shows qualitatively good agreement with the experimental data.

DOI: 10.1103/PhysRevB.65.155119

PACS number(s): 71.45.Lr, 75.30.Fv, 72.15.Eb, 72.15.Nj

I. INTRODUCTION

In the quasi-one-dimensional and quasi-two-dimensional systems the normal Fermi-liquid state is destroyed due to the quasiparticle interaction at low temperature and enters into one of four canonical states with energy gap: singlet superconductor, triplet superconductor, charge density wave (CDW), and spin-density wave (SDW).^{1,2}

However since the discovery of heavy fermion superconductors, organic superconductors, high- T_c superconductors, and Sr₂RuO₄, this simple picture has to be necessarily modified. First of all, most of these new superconductors are unconventional or nodal. The quasiparticle spectrum has no energy gap.³⁻⁵ Similarly some of the new CDW's and SDW's should be unconventional with no energy gap.⁶ Recently d -density wave state competing with superconductivity has been proposed to elucidate the phase diagram of cuprate superconductors.⁷ One of the signatures of these new states is insulating or semiconducting behavior but without clear energy gap. We shall call these new states unconventional CDW (or UCDW) and USDW.

Recently two of us⁸ have studied the thermodynamics and the optical response of USDW.^{8,9} The thermodynamics is very similar to the ones in d -wave superconductors.¹⁰ As to real systems, the low-temperature phase (LTP) of α -(BEDT-TTF)₂KHg(SCN)₄ abbreviated as α -(ET)₂ has not been clearly understood yet, where BEDT-TTF is bis(ethylenedithio)tetrathiafulvalene.¹¹⁻¹³ α -(ET)₂ salts can be separated into two groups: one superconducting and another with this mysterious LTP. The LTP does not exhibit x ray or nuclear magnetic resonance signals characteristic to conventional CDW or SDW and this property is naturally born out from the UDW model. This property is considered as hidden order in the literature.⁷ Further the response of the LTP in a magnetic field suggests that it is not SDW but more likely a kind of CDW. As we shall show later, the phase diagram of UCDW in a magnetic field is very

parallel to the one in d -wave superconductors,^{14,15} where the Pauli paramagnetism or the Zeeman energy dominates the magnetic interaction. Also it is known that in a magnetic field parallel to the conducting chain direction (in order to avoid the orbital effect) the UCDW splits into two regimes: the low-field regime where $\Delta(\mathbf{k}, \mathbf{r})$ is uniform in space and the high-field region where $\Delta(\mathbf{k}, \mathbf{r})$ varies periodically in space.^{16,17} In the first regime we shall show that the behavior of UCDW is exactly mapped to the one of d -wave superconductor when the Pauli paramagnetism or the Zeeman energy dominates the magnetic interaction.^{14,15} The second regime that corresponds to Fulde-Ferrell-Larkin-Ovchinnikov (FFLO) state,^{18,19} the mapping to d -wave superconductors²⁰ is not exact in general. In particular, the phase diagram for the quasi-one-dimensional UCDW will be different from the one expected for quasi-two-dimensional d -wave superconductors.

The object of the present paper is to extend the early analysis of UCDW⁸ and its threshold electric field²¹ in the presence of a magnetic field.²² Also, for simplicity, we focus on the Zeeman splitting (or the Pauli paramagnetic effect) due to an external magnetic field. Also, we limit ourselves to the case where $\Delta(\mathbf{k}, \mathbf{r})$ is independent of \mathbf{r} the space coordinates, where the thermodynamics of UCDW is the same as the one in d -wave superconductors. Then we can borrow the known results for the thermodynamics. These predictions can be readily tested by thermodynamic and scanning tunneling microscope measurements. The spin-lattice relaxation is evaluated showing clear features of the effect of magnetic field.

As to the electric conductivity we study the optical conductivity. At low temperature a clean optical gap develops below $\omega < 2\mu_B H$, which is smeared due to the possible thermal excitations at higher temperature. The divergent peak characteristic to the gap maximum⁸ remains sharp.

Then we shall consider the nonohmic conduction in UCDW. Earlier we have constructed the phase Hamil-

tonian for UCDW in the absence of magnetic field. Indeed, the data for the threshold electric field of α -(BEDT-TTF)₂KHg(SCN)₄ are available both as a function of temperature and magnetic field.^{23,24} Earlier we have compared our theoretical result for the threshold electric field to the one obtained in Ref. 23 as a function of temperature and we find a reasonable agreement if the three-dimensional weak-pinning limit applies.²¹

In the present paper we analyze the threshold electric-field data from Ref. 24 for $H=0$ T and $H=1$ T as a function of temperature. Again we obtain reasonable agreement.

These together with the magnetic phase diagram, the threshold electric field both $H=0$ T and 1 T provide us the convincing evidence that the LTP in α -(ET)₂ salts is UCDW.

II. PHASE DIAGRAM, DENSITY OF STATES, AND SPIN-LATTICE RELAXATION RATE

As a model we consider a quasi-one-dimensional interacting electron system described by the following Hamiltonian:

$$H = \sum_{\mathbf{k}, \sigma} [\varepsilon(\mathbf{k}) - \sigma \mu_B H] a_{\mathbf{k}, \sigma}^+ a_{\mathbf{k}, \sigma} + \frac{1}{2V} \sum_{\mathbf{k}, \mathbf{k}', \mathbf{q}} \tilde{V}(\mathbf{k}, \mathbf{k}', \mathbf{q}) a_{\mathbf{k}+\mathbf{q}, \sigma}^+ a_{\mathbf{k}, \sigma} a_{\mathbf{k}'-\mathbf{q}, \sigma'}^+ a_{\mathbf{k}', \sigma'}, \quad (1)$$

where $a_{\mathbf{k}, \sigma}^+$ and $a_{\mathbf{k}, \sigma}$ are, respectively, the creation and annihilation operators of an electron of momentum \mathbf{k} and spin σ , μ_B is the Bohr magneton, and H is the applied magnetic field, which is assumed to be parallel to the conducting chain in order to avoid the orbital effect. V is the volume of the sample, and the kinetic-energy spectrum on an orthorhombic lattice is given by

$$\varepsilon(\mathbf{k}) = -2t_a \cos(k_x a) - 2t_b \cos(k_y b) - 2t_c \cos(k_z c) - \mu, \quad (2)$$

where $t_a \gg t_b, t_c$. In the second term of Eq. (1) we consider the interaction between on site and nearest neighbor electrons as in Ref. 8. By moving from Bloch space to Wannier space, the Wannier function is well localized, leading to a significant dependence of the interaction matrix element on the incoming electron momenta \mathbf{k} and \mathbf{k}' . As a result the gap depends on the quasiparticle momentum like $\Delta(\mathbf{k}) = \Delta \cos(bk_y)$, for example. The phase diagram is the same as the one in a d -wave superconductor²⁵ without the FFLO state. At $T=0$ a first-order transition occurs to the normal state at $h=0.56\Delta_{00}$, where Δ_{00} is the zero-field zero-temperature order parameter and $h=\mu_B H$. The value of the gap is $0.92\Delta_{00}$ at the transition point. With decreasing field, the transition occurs at $h=0.41\Delta_{00}$, and the gap jumps from zero to $0.97\Delta_{00}$. For $T < 0.56T_{c0}$ (T_{c0} is the transition temperature at $h=0$) the transition remains first order, and hysteresis is observable somewhere between $0.41 < h/\Delta_{00} < 0.56$. In this region, the normal state becomes local minimum of the free energy, and depending on the direction of the change of the external field, the first-order transition oc-

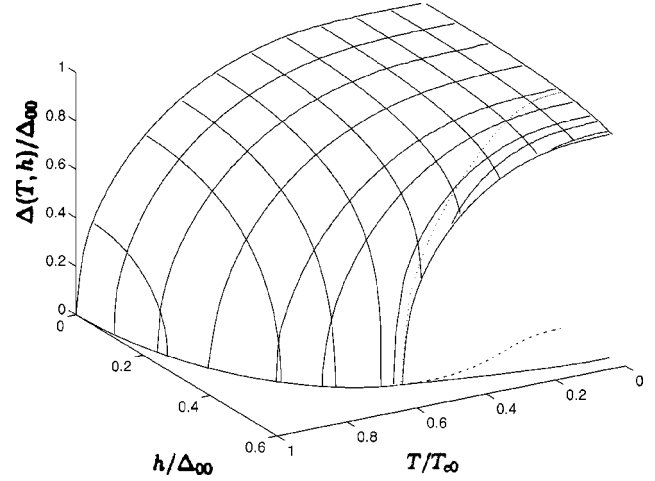


FIG. 1. Stereograph of the order parameter in the reduced temperature and field plane. The dotted line denotes the metastability line above which the normal state becomes local minimum of the free energy.

curs at smaller field approaching from the normal state than quitting the DW phase with increasing field. The presence of the first-order transition requires that the coefficient of the lowest-order term of Δ in the grand canonical potential vanishes:

$$\text{Re}\Psi''\left(\frac{1}{2} + \frac{ih}{2\pi T}\right) = 0, \quad (3)$$

which determines the bicritical point as $h/T \approx 1.91$, $T = 0.56T_{c0}$, and $h = 0.51\Delta_{00}$. By exceeding $T \approx 0.56T_{c0}$, the transition becomes second order at the bicritical point. The second-order phase diagram is given by

$$-\ln\left(\frac{T_c}{T_{c0}}\right) = \text{Re}\Psi\left(\frac{1}{2} + \frac{ih}{2\pi T_c}\right) - \Psi\left(\frac{1}{2}\right), \quad (4)$$

where T_c is the transition temperature at h magnetic field. It is worth noting that the phase diagram is modified at $T < 0.56T_{c0}$ and $h \sim 0.51\Delta_{00}$ because of the possibility of the FFLO regime what we excluded here for simplicity. The order parameter as a function of T and h is shown in Fig. 1. This phase diagram belongs to UCDW while for USDW it is completely different as in the case of conventional CDW and SDW. In a conventional SDW the effect of the Zeeman term is completely canceled out^{26–28} due to spin flop: the spins are oriented perpendicular to the magnetic field because of the anisotropy of the spin space. Since in the case of USDW the spin susceptibility⁸ retains the anisotropy found in conventional SDW, the Pauli term has no effect on USDW. Consequently the transition temperature is not expected to change. The only field effect is due to the orbital effect, which we ignore in the present paper. The effect discussed in Ref. 29 may be of importance, but this is beyond the scope of the present paper.

The quasiparticle density of states (DOS) averaged over the spin is obtained as¹⁴

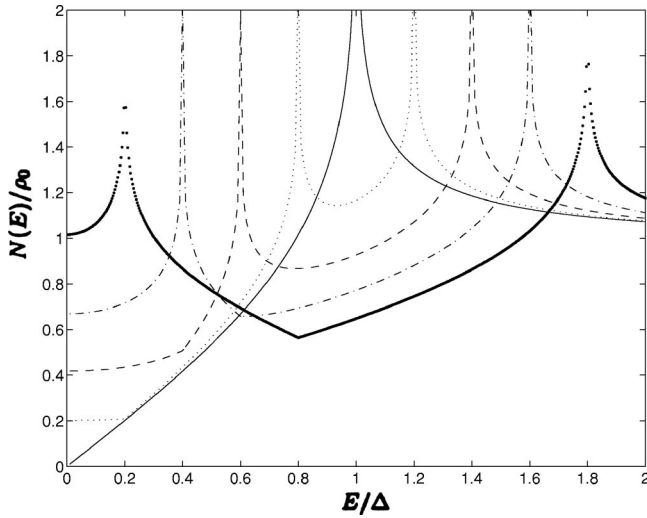


FIG. 2. The density of states is shown as a function of E/Δ for $h/\Delta=0$ (solid line), 0.2 (thin dotted line), 0.4 (dashed line), 0.6 (dashed-dotted line), and 0.8 (thick dotted line).

$$N(E) = \frac{1}{2}[\rho(E+h) + \rho(E-h)], \quad (5)$$

where $\rho(E)$ is the density of states in the absence of magnetic field, and is given by⁸ $\rho(E)/\rho_0(0) = (2|E|/\pi|\Delta|)K(|E|/|\Delta|)$ if $|E| < |\Delta|$, and $\rho(E)/\rho_0(0) = (2/\pi)K(|\Delta|/|E|)$ if $|E| > |\Delta|$. $K(z)$ is the complete elliptic integral of the first kind. The density of states per spin is given by $\rho(E \pm h)$, where the upper and lower sign belongs to down and up spins, respectively. As h increases, the valley in the averaged DOS at the Fermi surface is filled in. Also, the divergent peaks at $\pm\Delta$ split into four new peaks at $\pm\Delta \pm h$. Interestingly, at $h=\Delta$ the density of states is divergent at the Fermi surface, resulting in an unexpected change of slope in the spin-lattice relaxation rate, for example. These properties can be seen in Fig. 2.

As a direct use of the obtained density of states per spin, the spin susceptibility and the spin-lattice relaxation rate can be evaluated from:

$$\frac{\chi(T, h)}{\chi_0} = \frac{1}{4T} \int_0^\infty dE \frac{\rho(E+h) + \rho(E-h)}{\rho_0} \text{sech}^2 \frac{E}{2T}, \quad (6)$$

$$\frac{R(T, h)}{R_N} = \frac{1}{2T} \int_0^\infty dE \frac{\rho(E+h)\rho(E-h)}{\rho_0^2} \text{sech}^2 \frac{E}{2T}. \quad (7)$$

At $T=0$ they are given by the following formulas:

$$\frac{\chi(0, h)}{\chi_0} = \frac{2h}{\pi\Delta} K\left(\frac{h}{\Delta}\right) \sim h, \quad (8)$$

$$\frac{R(0, h)}{R_N} = \left(\frac{2hK(h\Delta)}{\pi\Delta}\right)^2 \sim h^2, \quad (9)$$

which results in a linear magnetic field dependence almost in the entire h range for the spin susceptibility and a quadratic

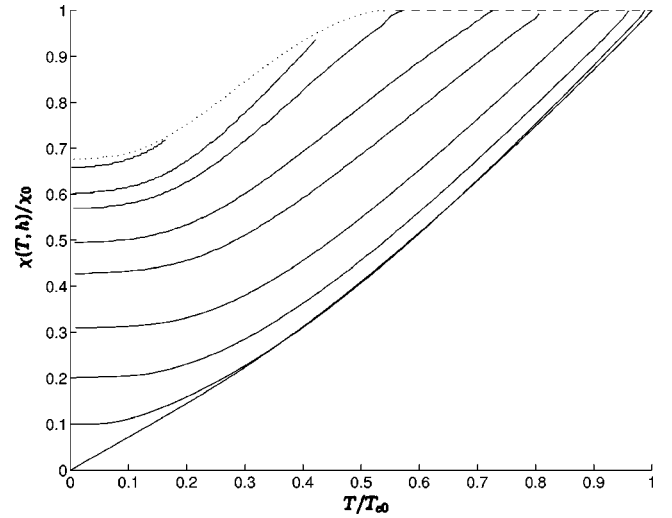


FIG. 3. The spin susceptibility is shown as a function of the reduced temperature for $h/\Delta=0, 0.1, 0.2, 0.3, 0.4, 0.45, 0.5, 0.52$, and 0.55 with endpoints from right to left. The dashed (dotted) line represents $\chi(T, h)$ along the second- (first-) order phase boundary.

one for $R(0, h)$. In the low temperature and small magnetic field limit, $\chi(T, h)$ is approximated as¹⁴

$$\frac{\chi_s(T, h)}{\chi_0} = \begin{cases} 2 \ln(2) \frac{T}{\Delta_{00}} + \frac{h^2}{4T\Delta_{00}}, & \frac{h}{T} \ll 1, \\ \frac{h}{\Delta_{00}}, & \frac{h}{T} \gg 1. \end{cases} \quad (10)$$

The spin susceptibility is shown as a function of the reduced temperature and magnetic field in Figs. 3 and 4. At $h=0$, the low-temperature behavior of the relaxation rate is identified as

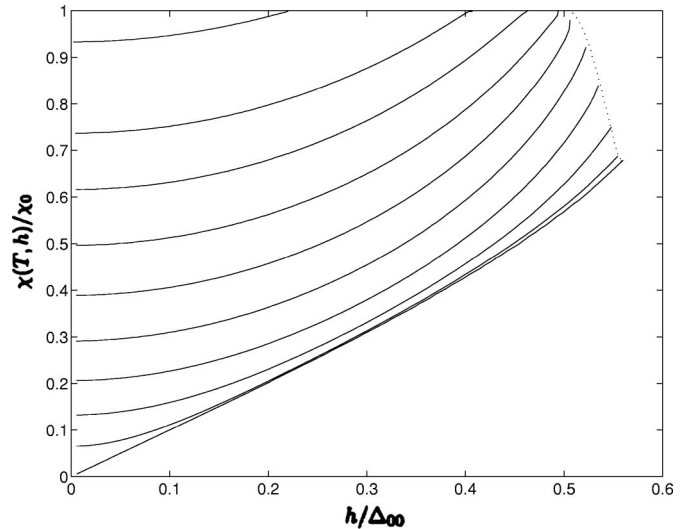


FIG. 4. The spin susceptibility is shown as a function of the magnetic field for $T/T_0=0, 0.1, 0.2, 0.3, 0.4, 0.5, 0.6, 0.7, 8$, and 0.95 with endpoints from right to left. The dashed (dotted) line accounts for $\chi(T, h)$ along the second- (first-) order phase boundary.

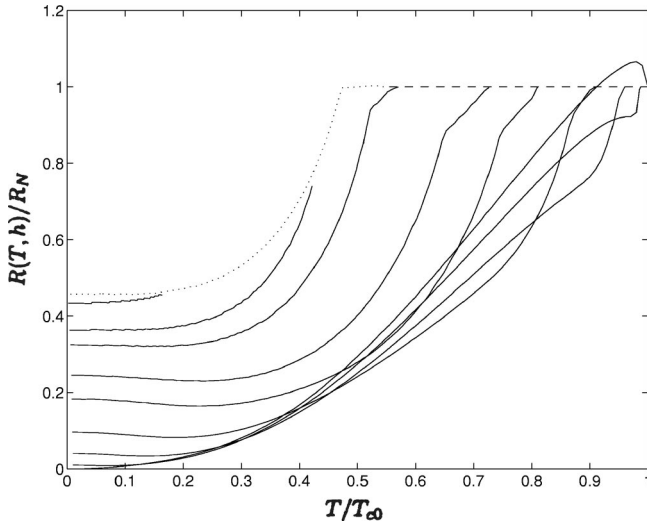


FIG. 5. The spin-lattice relaxation rate is shown as a function of the reduced temperature for $h/\Delta = 0, 0.1, 0.2, 0.3, 0.4, 0.45, 0.5, 0.52$, and 0.55 with endpoints from right to left. The dashed (dotted) line represents $R(T, h)$ along the second- (first-) order phase boundary.

$$\frac{R(T, 0)}{R_N} = \frac{1}{3} \left(\frac{\pi T}{\Delta} \right)^2, \quad (11)$$

while at $h=0$ close to T_{c0} the small peak starts as

$$\frac{R(T, 0)}{R_N} = 1 + 0.85 \sqrt{1 - \frac{T}{T_{c0}}}, \quad (12)$$

which can be regarded as the reminiscent of the divergent peak in Maniv's expression³⁰ for the relaxation rate of conventional density waves. At arbitrary T and h , the spin-lattice relaxation rate is evaluated numerically, and is shown in Figs. 5 and 6.

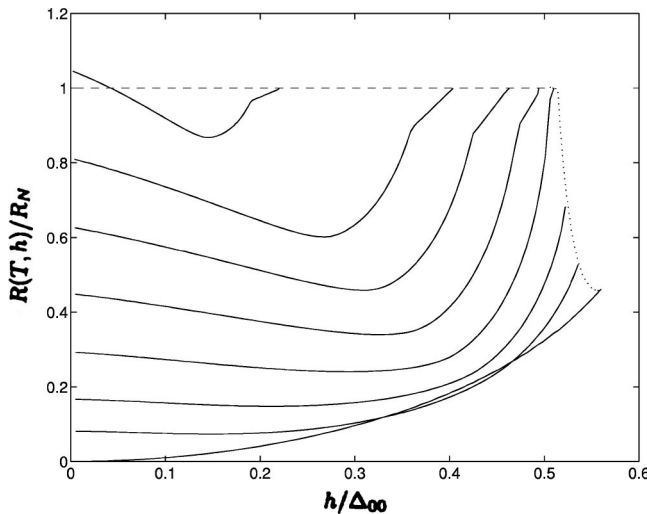


FIG. 6. The spin-lattice relaxation rate is shown as a function of the magnetic field for $T/T_{c0} = 0, 0.3, 0.4, 0.5, 0.6, 0.7, 8$ and 0.95 with endpoints from right to left. The dashed (dotted) line accounts for $R(T, h)$ along the second- (first-) order phase boundary.

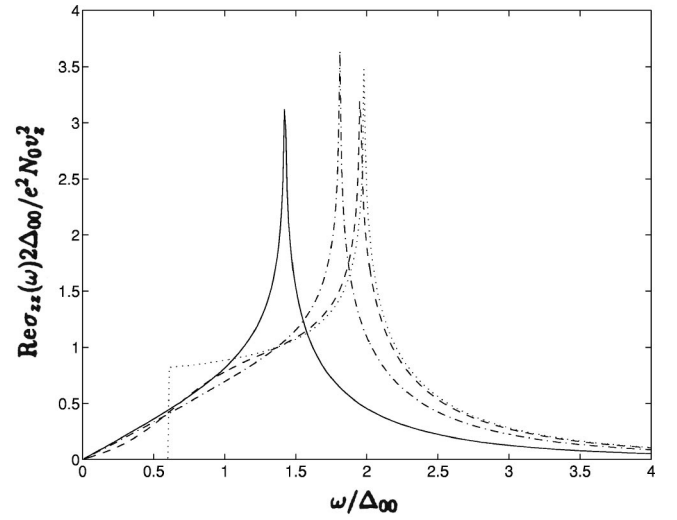


FIG. 7. The real part of the complex conductivity in the z direction with unconventional gap in the y direction is shown at $h = 0.3\Delta_{00}$ for $T/T_c = 0$ (dotted line), 0.25 (dashed line), 0.5 (dashed-dotted line), and 0.75 (solid line). Note that the same curves belong to the quasiparticle part of $\sigma_{xx}(\omega)$ by changing v_z to v_F .

The sudden change of slope close to the actual transition temperature occurs at $h = \Delta(T, h)$ when a new divergence steps into the integral.

III. OPTICAL CONDUCTIVITY

The optical conductivity contains relevant informations about the quasiparticle and collective excitation spectrum of density waves.² Here we explore the temperature and magnetic field dependence of the quasiparticle part of the conductivity without the effect of impurities. In the chain direction the optical conductivity consists of a Dirac delta peak at zero frequency due to the collective contributions as it is the case in conventional DW, if no damping is present for the electrons. In the perpendicular directions the quasiparticle contribution gives to total optical conductivity, since no collective contribution is expected in this case. The regular part of the optical conductivity (without the Dirac delta) is obtained as

$$\text{Re}\sigma_{\alpha\beta}^{\text{reg}}(\omega, h) = \text{Re}\sigma_{\alpha\beta}^{\text{reg}, 0}(\omega) \frac{1 - \tanh(h/T)^2}{1 - \tanh(\omega/T)^2 \tanh(h/T)^2}, \quad (13)$$

where $\text{Re}\sigma_{\alpha\beta}^{\text{reg}, 0}(\omega)$ is the optical conductivity⁸ at $h=0$ in which the magnetic field enters only through $\Delta(T, h)$, hence the explicitly magnetic field dependent term can be separated.

We show the optical conductivity in Figs. 7, 8, 9 for gap functions $\Delta(\mathbf{k}) = \Delta \sin(bk_y)$ or $\Delta(\mathbf{k}) = \Delta \cos(bk_y)$ for $T/T_c = 0, 0.25, 0.5$, and 0.75 at $h = 0.3\Delta_{00}$. This particular magnetic field value is chosen because it is in the bulk of the phase diagram so in this respect the general behavior of the optical conductivity can be seen in the figures. Also as we will show later, the threshold electric field belonging to this

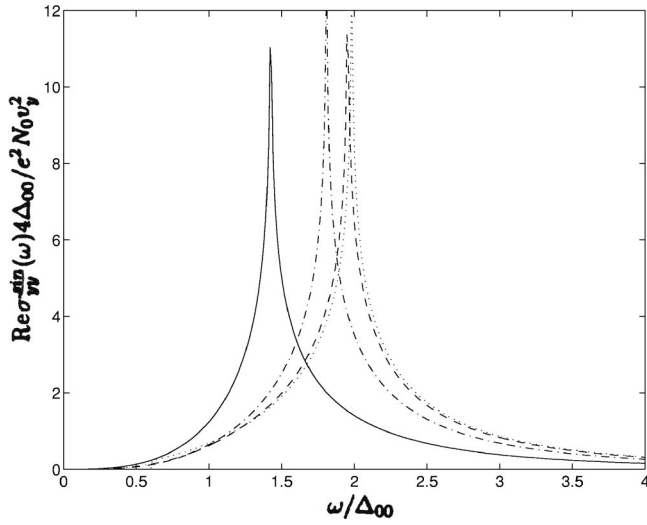


FIG. 8. The real part of the complex conductivity for a sinusoidal gap in the y direction is shown at $h=0.3\Delta_{00}$ for $T/T_c=0$ (dotted line), 0.25 (dashed line), 0.5 (dashed-dotted line), and 0.75 (solid line).

particular h value describes well the experimentally obtained threshold electric field at $H=1$ T.

At $T=0$, $h \neq 0$ a clean optical gap ($=2h$) develops in the optical conductivity because the optical transfer from occupied to empty states requires a minimum of $2h$ energy. Consequently, the sum rule seems to be violated since a lot of optical weight is missing below the optical gap. But the missing oscillator strength is transferred to the weight of the Dirac delta at zero frequency even at $T=0$. As a result, in real systems where impurities are present, we expect a broadening of the Dirac delta into a Lorentzian like curve dominated at higher frequencies by the broadened quasiparticle contribution (with no sharp peaks). In the chain direction, the

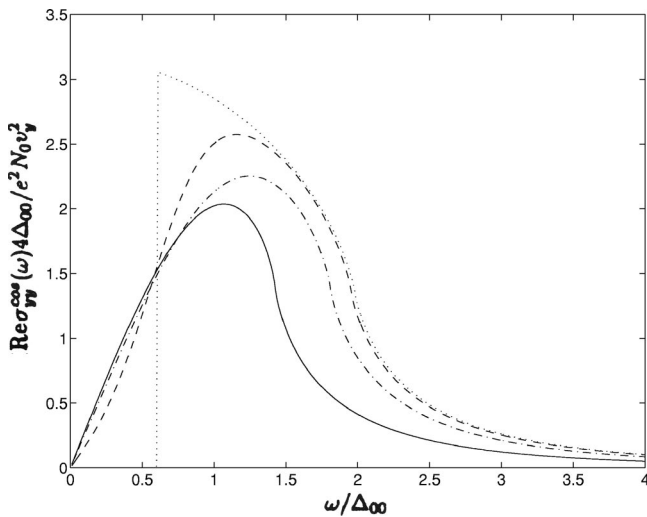


FIG. 9. The real part of the complex conductivity for a cosinusoidal gap in the y direction is shown at $h=0.3\Delta_{00}$ for $T/T_c=0$ (dotted line), 0.25 (dashed line), 0.5 (dashed-dotted line), and 0.75 (solid line).

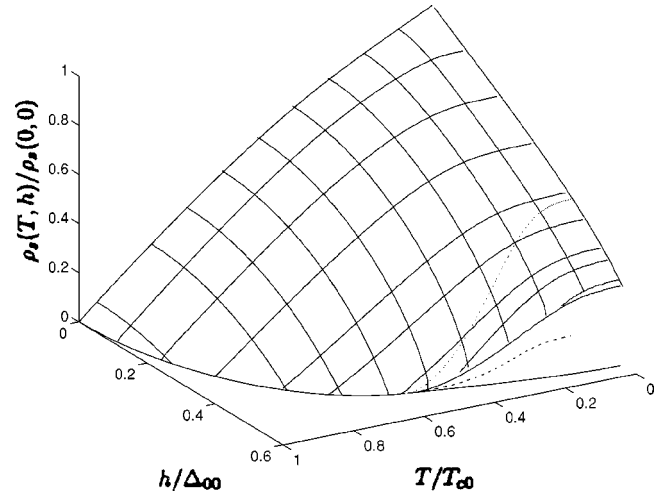


FIG. 10. Stereograph of the condensate density in the reduced temperature and field plane. The dotted line denotes the metastability line above which the normal state becomes local minimum of the free energy.

Dirac delta peak is expected to be broadened and more importantly to move to the pinning frequency as in conventional DW.

The logarithmically divergent peak at $\omega=2\Delta(T, h)$ in Figs. 7 and 8 is the consequence of the fact that the distance of the divergent peaks in the density of state per spin is exactly $2\Delta(T, h)$. However, this peak in Fig. 9 is suppressed because of the zero velocity of the electrons at the gap maximum.

IV. PHASE HAMILTONIAN AND THE THRESHOLD ELECTRIC FIELD

To study the threshold electric-field phenomenon, the pinning of the density wave is necessary. The simplest source of pinning is to consider the effect of nonmagnetic impurities as in Ref. 21. One consequence of the impurities is the finite lifetime of quasiparticles as it was mentioned in the preceding section. Another important effect of the pinning is the finite threshold electric field at which the sliding motion of the condensate sets in. It is the most convenient to formulate the threshold electric field in terms of the phase Hamiltonian, which is given as^{31,32}

$$H(\Phi) = \int d^3r \left\{ \frac{1}{4} N_0 f \left[v_F^2 \left(\frac{\partial \Phi}{\partial x} \right)^2 + v_b^2 \left(\frac{\partial \Phi}{\partial y} \right)^2 + v_c^2 \left(\frac{\partial \Phi}{\partial z} \right)^2 + \left(\frac{\partial \Phi}{\partial t} \right)^2 - 4 v_F e E \Phi \right] + V_{imp}(\Phi) \right\}, \quad (14)$$

where N_0 is the density of states in the normal state at the Fermi surface per spin, $f = \rho_s(T, h)/\rho_s(0, 0) = 1 - \chi(T, h)/\chi_0$ where $\rho_s(T, h)$ is the condensate density¹⁴ and E is an electric field applied in the x direction. Here v_F , v_b , and v_c are the characteristic velocities of the quasi-one-dimensional electron system in the three spatial directions.

For UDW the condensate density is the same as the superfluid density in d -wave superconductors and is shown in Fig. 10.

We may think of Eq. (14) as a natural extension of the Fukuyama-Lee-Rice (FLR) Hamiltonian^{33,34} for UCDW and for $T \neq 0$, $H \neq 0$, and for three spatial directions.

The pinning potential is obtained as

$$V_{imp}(\Phi) = -\frac{8V_0V_yN_0^2}{\pi} \sum_j \cos[2(\mathbf{Q}\mathbf{R}_j + \Phi(\mathbf{R}_j))]\Delta(T, h) \\ \times \int_0^1 \frac{1}{2} \left(\tanh \frac{\beta[\Delta(T, h)x + h]}{2} \right. \\ \left. + \tanh \frac{\beta[\Delta(T, h)x - h]}{2} \right) \\ \times E(\sqrt{1-x^2})[K(x) - E(x)]dx, \quad (15)$$

where \mathbf{R}_j is an impurity site, $K(z)$ and $E(z)$ are the complete elliptic integrals of the first and second kind, respectively. In obtaining Eq. (15) we assumed a nonlocal impurity potential:²¹

$$U(\mathbf{Q} + \mathbf{q}) = V_0 + \sum_{i=y,z} V_i \cos(q_i \delta_i). \quad (16)$$

Then following FLR,^{33,34} in the strong pinning limit the threshold electric field at $T=0$ is given by

$$E_T^S(0, h) = \frac{2k_F}{e} \frac{n_i}{n} N_0^2 V_0 V_y \frac{16}{\pi} \frac{\Delta(0, h)}{\rho_s(0, h)} \int_{h/\Delta_{00}}^1 E(\sqrt{1-x^2}) \\ \times [K(x) - E(x)]dx, \quad (17)$$

and for general temperature it is obtained as

$$\frac{E_T^S(T, h)}{E_T^S(0, 0)} = \frac{\rho_s(0, 0)}{\rho_s(T, h)} \frac{\Delta(T, h)}{\Delta_{00}} \frac{1}{0.5925} \\ \times \int_0^1 \frac{1}{2} \left(\tanh \frac{\beta[\Delta(T, h)x + h]}{2} \right. \\ \left. + \tanh \frac{\beta[\Delta(T, h)x - h]}{2} \right) E(\sqrt{1-x^2}) \\ \times [K(x) - E(x)]dx, \quad (18)$$

where 0.5925 is the value of the integral in the second line of Eq. (18) at $T=0$ and $h=0$.

At low temperature using Eq. (10), E_T^S is well approximated by

$$\frac{E_T^S(T, h)}{E_T^S(0, 0)} \approx \frac{\rho_s(0, 0)}{\rho_s(T, h)} = \begin{cases} 1 + 2 \ln(2) \frac{T}{\Delta_{00}} + \frac{h^2}{4T\Delta_{00}}, & \frac{h}{T} \ll 1, \\ 1 + \frac{h}{\Delta_{00}}, & \frac{h}{T} \gg 1 \end{cases} \quad (19)$$

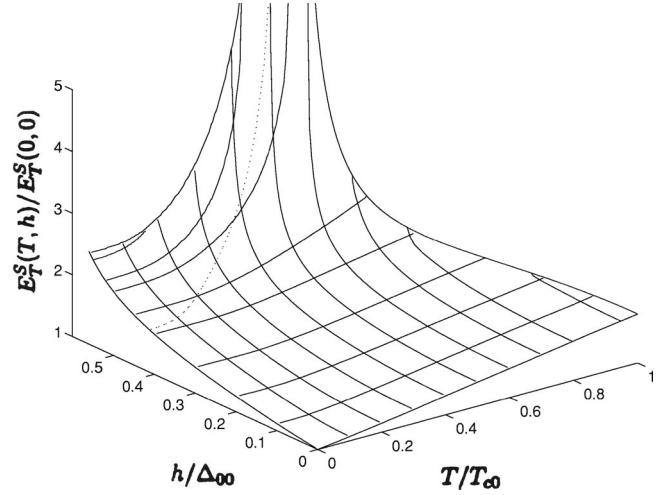


FIG. 11. The threshold electric field in the strong pinning limit is plotted as a function of the reduced temperature and field. The dashed line is the threshold field belonging to the metastability line.

in the $h, T \ll \Delta_{00}$ range.¹⁴ For $T > 0.56T_{c0}$, along the second-order phase boundary the threshold electric field is obtained from Eq. (18) in the $\Delta \rightarrow 0$ limit as

$$\frac{E_T^S(T, h)}{E_T^S(0, 0)} = -\frac{\text{Re}\Psi' \left(\frac{1}{2} + \frac{ih}{2\pi T} \right)}{\text{Re}\Psi'' \left(\frac{1}{2} + \frac{ih}{2\pi T} \right)} \frac{T}{\Delta_{00}} \frac{\pi^3}{4 \times 0.5925}, \quad (20)$$

which is divergent at the bicritical point (possibly tricritical with the FFLO state). This divergence is not an artifact because the vanishing denominator coincides with the condition for the presence of first-order phase boundary, as it was already discussed in Eq. (3). As a result, the threshold electric field close to the bicritical point is given by

$$\frac{E_T^S(T, h)}{E_T^S(0, 0)} = \frac{1.12}{1.91 - h/T} \quad (21)$$

approaching along the second-order phase boundary. The presence of FFLO state would not affect this behavior since it may appear below $0.56T_{c0}$, consequently this new phase does not change quantities evaluated along the second-order phase boundary. We show the threshold electric field as a function of the temperature and the magnetic field in Fig. 11 in the strong pinning limit.

The weak-pinning limit is more appropriate for high quality crystals. Then we obtain for a three-dimensional system,

$$\frac{E_T^W(T, h)}{E_T^W(0, 0)} = \left(\frac{E_T^S(T, h)}{E_T^S(0, 0)} \right)^4. \quad (22)$$

$E_T^W(T, h)$ is plotted as a function of temperature and magnetic field in Figs. 12 and 13, respectively.

At small but increasing fields, the enhancement of the threshold electric field at the transition temperature relative to the $T=0$ value becomes smaller due to the initial linear decrease of the condensate density versus h at $T=0$. At low

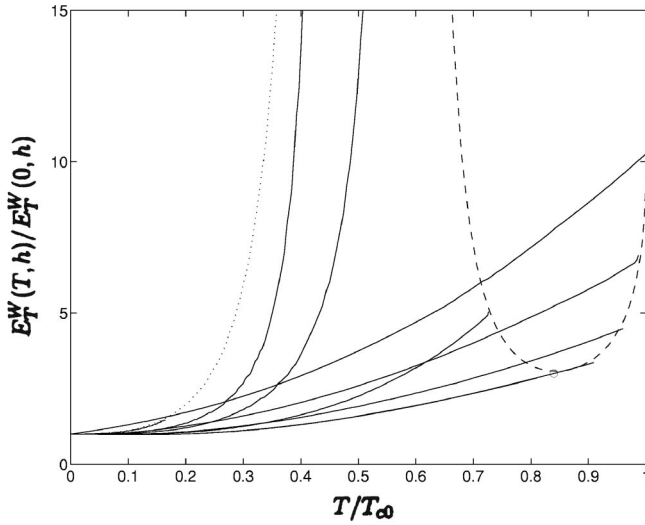


FIG. 12. The threshold electric field in the weak pinning limit is plotted as a function of the reduced temperature for $h/\Delta_{00}=0, 0.1, 0.2, 0.3, 0.4, 0.45, 0.5, 0.52$, and 0.55 with endpoints from right to left. The circle represents the end of the $h=0.4\Delta_{00}$ curve, which is very close to the $h=0.3\Delta_{00}$ one. The dashed line accounts for the threshold field along the second-order phase boundary while the dotted line accounts for the one along the first-order phase boundary.

temperature $E_T^W(T, h)$ increases with h almost linearly. Further $E_T^W(T, h)$ diverges for $T \approx 0.56T_{c0}$ when the magnetic transition changes from second order to first order.

As a direct application of the theory to real materials, we present the threshold electric field data²⁴ in α -(ET)₂ salts in the presence of magnetic field together with our prediction in Fig. 14. At zero field the agreement is excellent. At H

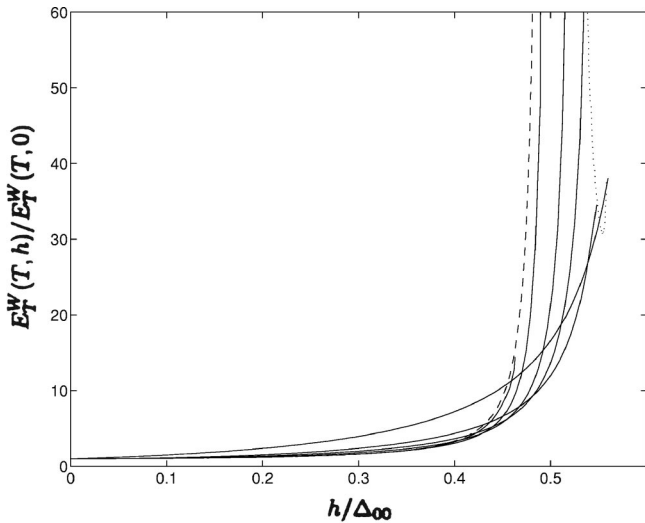


FIG. 13. The threshold electric field in the weak pinning limit is plotted as a function of the magnetic field for $T/T_{c0}=0, 0.2, 0.3, 0.4, 0.6$, and 0.7 with endpoints from right to left. The dashed line accounts for the threshold field along the second-order phase boundary while the dotted line accounts for the one along the first-order phase boundary.

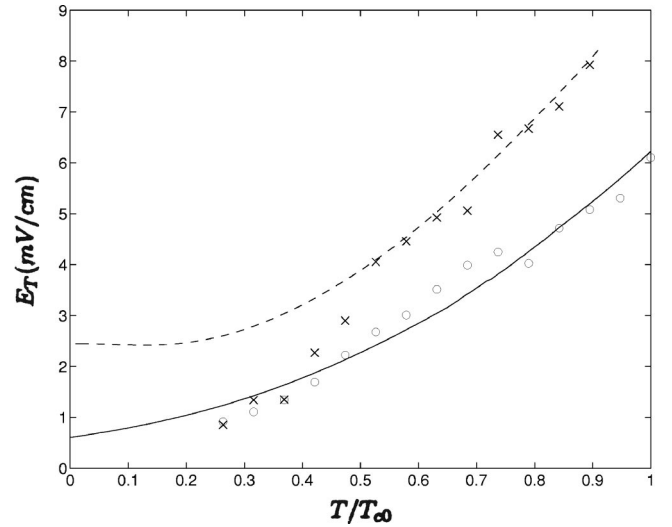


FIG. 14. The theoretical and experimental threshold electric field are plotted as a function of the reduced temperature. The measured E_T in the α -(ET)₂ salts²⁴ is shown for $H=0$ T (open circles) and $H=1$ T (crosses). The solid (dashed) line represents the theoretical curve at $h/\Delta_{00}=0$ ($h=0.3\Delta_{00}$).

$=1$ T, the agreement at low temperatures is qualitatively good with the $h=0.3\Delta_{00}$ curve as far as the increasing tendency is concerned, while close to the transition temperature the matching is remarkable again. By fitting our theoretical curves to the experimental data, the only fitting parameter, $E_T(0,0)$ was determined first from the $H=0$ case. Then by changing the magnetic field, $h=0.3\Delta_{00}$ was found to be the closest to the measured threshold electric field at $H=1$ T. As a result, Δ_{00} turns out to be of the order of a few kelvins, which falls of the same order of magnitude as the transition temperature ($T_c \sim 8$ K). The remaining discrepancy of the numerical values may arise from the neglect of the Fermi-liquid renormalization of the Bohr magneton.

At the same time, the strong H dependence of the threshold electric field at $T=2.2$ K referred to in Ref. 23 appears to be consistent with the present result, though no details are available. Clearly, these are the only available data at the moment, so we should really need more experiments in this field to make more decisive statements. Unfortunately, the present result does not apply for $T < 0.56T_{c0}$ and $h \gtrsim 0.51\Delta_{00}$ due to the presence of the FFLO regime. Nevertheless, the present result can be tested in a wide range of the H - T phase diagram of the LTP in α -(ET)₂ salts. The effect of the FFLO state and the related threshold electric field is beyond the scope of the present paper.

V. CONCLUDING REMARKS

In this paper we have extended our earlier analysis on unconventional density waves⁸ in the presence of magnetic field. The magnetic field is introduced as the Zeeman splitting. The phase diagram is found to be identical to the one in a d -wave superconductor²⁵ without the FFLO state. The density of states averaged over the spins exhibit four sharp peaks at $\pm\Delta \pm h$ instead of the usual peaks at $\pm\Delta$. The enhance-

ment of the spin susceptibility in the presence of magnetic field clearly shows the destructive effect of the applied field and can be readily accessible from Knight-shift measurements. The cusplike behavior of the spin-lattice relaxation rate close to T_c is a unique property of this system together with the h^2 dependence at $T=0$. The optical conductivity in the perpendicular directions properly distinguishes between the possible gap structures. The appearance of the clean optical gap ($\sim h$) with the applied field at very low temperatures differs from the conventional density wave scenario where the magnetic field has no effect on the optical gap for $h < 2\Delta$ in either perpendicular directions. The present model predicts very strong H dependence of the threshold electric field, even divergent behavior at the bicritical point, which should be readily accessible experimentally.

The so-called hidden order, the missing of any obvious long-range order together with robust thermodynamic features of phase transitions makes UCDW a very likely candidate for the ground state of the α -(ET)₂ salts. Moreover the destruction of the UCDW phase in the presence of applied magnetic field coincides with experimental observations.^{11,13} The detection of the threshold electric field in the α -(ET)₂

salts excludes all the possible non-density-wave like ground states. E_T in conventional CDW and SDW theories is not in agreement with experiments on α -(ET)₂ salts. The former predicts a divergent peak at the transition temperature while the latter gives an almost temperature-independent threshold electric field. On the other hand, E_T in UCDW describes the experimental data on α -(ET)₂ salts as it can be seen either in Ref. 21 or in Fig. 14. The strong H dependence of threshold electric field agrees well with experimental results, which surely strengthen our proposal that the LTP of α -(ET)₂ salts should be UCDW.

ACKNOWLEDGMENTS

We would like to thank Bojana Korin-Hamzić for useful discussions on possible H dependence of the threshold electric field. We thank also Takahiko Sasaki for providing us with the experimental data. This work was supported by the Hungarian National Research Fund under Grants Nos. OTKA T032162 and T037451, and by the Ministry of Education under Grant No. FKFP 0029/1999.

-
- ¹J. Sólyom, *Adv. Phys.* **28**, 201 (1979).
²G. Grüner, *Density Waves in Solids* (Addison-Wesley, Reading, 1994).
³H. Won and K. Maki, in *Symmetry and Pairing in Superconductors*, edited by M. Ausloos and S. Kruchinin (Kluwer, Dordrecht, 1999).
⁴C.C. Tsuei and J.R. Kirtley, *Rev. Mod. Phys.* **72**, 969 (2000).
⁵D.J.V. Harlingen, *Rev. Mod. Phys.* **67**, 515 (1995).
⁶A.A. Nersisyan, G.I. Japaridze, and I.G. Kimeridze, *J. Phys.: Condens. Matter* **3**, 3353 (1991).
⁷S. Chakravarty, R.B. Laughlin, D.K. Morr, and C. Nayak, *Phys. Rev. B* **63**, 094503 (2001).
⁸B. Dóra and A. Virosztek, *Eur. Phys. J. B* **22**, 167 (2001).
⁹B. Dóra and A. Virosztek, *J. Phys. IV* **9**, Pr10 239 (1999).
¹⁰H. Won and K. Maki, *Phys. Rev. B* **49**, 1397 (1994).
¹¹P. Christ, W. Biberacher, M.V. Kartsovnik, E. Steep, E. Balthes, H. Weiss, and H. Müller, *JETP Lett.* **71**, 303 (2000).
¹²J. Singleton, *Rep. Prog. Phys.* **63**, 1161 (2000).
¹³D. Andres, M.V. Kartsovnik, W. Biberacher, H. Weiss, E. Balthes, H. Müller, and N. Kushch, *Phys. Rev. B* **64**, 161104(R) (2001).
¹⁴H. Won, H. Jang, and K. Maki, cond-mat/9901252 (unpublished).
¹⁵H. Won, H. Jang, and K. Maki, *Physica B* **281-282**, 944 (2000).
¹⁶D. Zanchi, A. Bjelis, and G. Montambaux, *Phys. Rev. B* **53**, 1240 (1996).
¹⁷A. Bjelis, D. Zanchi, and G. Montambaux, *J. Phys. IV* **9**, Pr10 203 (1999).
¹⁸P. Fulde and R.A. Ferrell, *Phys. Rev.* **35**, A550 (1964).
¹⁹A.I. Larkin and N. Ovchinnikov *Zh. Éksp. Teor. Fiz.* **47**, 1136 (1964) [*Sov. Phys. JETP* **20**, 762 (1965)].
²⁰K. Maki and H. Won, *Czech. J. Phys.* **46**, S2 1035 (1996).
²¹B. Dóra, A. Virosztek, and K. Maki, *Phys. Rev. B* **64**, 041101(R) (2001).
²²B. Dóra, A. Virosztek, and K. Maki, *Curr. Appl. Phys.* **1**, 313 (2001).
²³M. Basletić, B. Korin-Hamzić, M.V. Kartsovnik, and H. Müller, *Synth. Met.* **120**, 1021 (2001).
²⁴T. Fujita, T. Sasaki, N. Yoneyama, N. Kobayashi, and T. Fukase, *Synth. Met.* **120**, 1077 (2001).
²⁵K. Yang and S.L. Sondhi, *Phys. Rev. B* **57**, 8566 (1998).
²⁶K. Yamaji, *Synth. Met.* **13**, 29 (1986).
²⁷A. Virosztek, L. Chen, and K. Maki, *Phys. Rev. B* **34**, 3371 (1986).
²⁸D. Poilblanc, M. Heritier, G. Montambaux, and P. Lederer, *J. Phys. C* **19**, L321 (1986).
²⁹A. Bjelis and B. Zanchi, *Phys. Rev. B* **49**, 5968 (1994).
³⁰T. Maniv, *Solid State Commun.* **43**, 47 (1982).
³¹K. Maki and A. Virosztek, *Phys. Rev. B* **39**, 9640 (1989).
³²K. Maki and A. Virosztek, *Phys. Rev. B* **42**, 655 (1990).
³³H. Fukuyama and P.A. Lee, *Phys. Rev. B* **17**, 535 (1978).
³⁴P.A. Lee and T.M. Rice, *Phys. Rev. B* **19**, 3970 (1979).